SKELETONIZATION USING SSM OF THE DISTANCE TRANSFORM

Longin Jan Latecki[1], Quan-nan Li[2], Xiang Bai[2], Wen-yu Liu[2]

[1] Temple University, Philadelphia, USA
[2] HuaZhong University of Science and Technology, Wuhan, China

ABSTRACT

This paper proposes a new approach for skeletonization based on the skeleton strength map (SSM) caculated by Euclidean distance transform of a binary image. After the distance transform and gradient are computed, isotropic diffusion is performed on the gradient vector field and the skeleton strength map is computed from the diffused vector field. A critical point set is then selected from local maxima of the SSM. The critical points are located on significant visual parts of the object. The skeleton is obtained by connecting the critical points with geodesic paths. This approach overcomes intrinsic drawbacks of distance transform based skeletons, since it yields stable and connected skeletons without losing significant visual parts.

Index terms—Skeletonization, gradient vector field, isotropic diffusion, distance transform, skeleton strength map (SSM)

1. INTRODUCTION

Skeleton, also known as Medial Axis, is defined by the grassfire model [3] or with centers of maximum disks [4]. It is an important descriptor of object since it preserves the topological and geometrical properties. It is important for object representation and recognition in different areas, such as image retrieval and computer graphics, character recognition, image processing, and analysis of biomedical images.

Broadly used skeletonization approaches can classified in four types: thinning algorithms, discrete domain algorithms based on the Voronoi diagram, algorithms based on distance transform, and algorithms based on mathematical morphology. Many algorithms based on distance transform compute the skeleton by detecting ridges on the distance transform surface [5][6][7]. Those algorithms can ensure the accurate localization of skeleton points but neither connectivity nor completeness, that is, the branches extracted may be disconnected and may not be able to represent all the significant visual parts.

Siddiqi et al. [8] measure the average outward flux of the vector field that underlies the Hamiltonian system and combine the flux measurement with a homotopy preserving thinning process applied in a discrete lattice. This approach leads to a robust and accurate algorithm for computing skeletons in 2D as well as 3D. However, the error in calculating the flux is both limited by the pixel resolution and also proportional to the curvature of the boundary evolution front. This makes the exact location of endpoints difficult. Torsello et al. [9] overcome this problem by taking into account variations of density due to boundary curvature and eliminating the curvature contribution to the error. Aslan and Tari [10] present an unconventional approach for shape recognition using unconnected skeletons in the coarse level. This approach can leads to stable skeletons in the presence of boundary deformations, however, the obtained skeletons do not represent any shape details.

The skeletons computed by the proposed approach are localized accurately in the middle between corresponding boundary curves in accord with the definition of medial axis. Moreover, the computed skeletons are guaranteed to be connected and complete (all significant visual branches are present). Details of the proposed approach are presented in Section 2. Experimental results that demonstrate the above properties are given in Section 3.

2. EXTRACTION OF SKELETONS

The basic idea of this approach is to select critical points from the skeleton strength map (SSM) and connect them by geodesic paths computed with Dijkstra's shortest path algorithm [12]. The skeletonization process is demonstrated in Fig. 1.
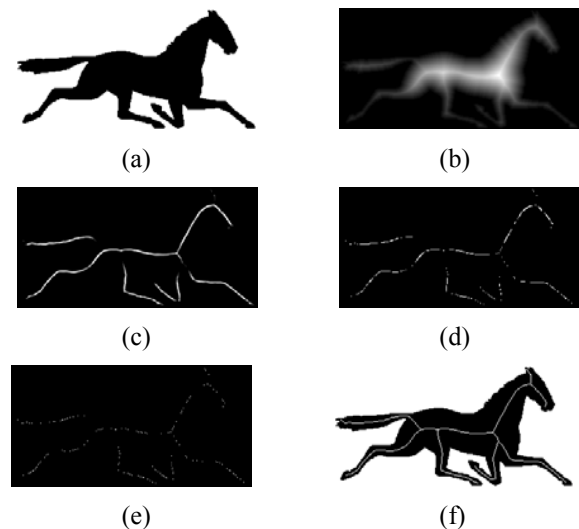

(a)   (b)

(c)   (d)

(e)   (f)

Fig. 1 Illustration of skeletonization by this approach. (a) is the original image, (b) the distance transform of (a), (c) is the SSM, (d) is the local maxima, (e) is the critical point set extracted from (d), (f) is the final skeleton.

Critical point selection from the SSM yields a complete set of critical points so that this approach does not miss visual parts. Finally, the critical points are connected with geodesic paths, which guarantees the connectivity of the obtained skeleton.

2.1. Isotropic diffusion of the gradient vector field of the Euclean distance transform

Distance transform $dt(\vec{r})$ is the distance of an interior point $\vec{r}$ to the nearest boundary point. It is a scalar field and we can easily compute its gradient vector. However, here we first compute $f(\vec{r}) = 1 - \|\nabla G_\delta(\vec{r}) * dt(\vec{r})\|$ to replace $dt(\vec{r})$, where $G_\delta(\vec{r})$ is the Gaussian kernel function, δ is its standard covariance and $*$ is the convolution operator. $f(\vec{r})$ can be treated as an inverted version of the smoothed gradient magnitude of $dt(\vec{r})$. The main advantage of working with $f(\vec{r})$ in place of $dt(\vec{r})$ is based on the fact the relative value between skeleton point and it neighbors is significantly larger for $f(\vec{r})$ than for $dt(\vec{r})$. Therefore, we work with the gradient of $f(\vec{r})$:

$$(u_0, v_0) = \nabla f = (\frac{\partial f}{\partial x}, \frac{\partial f}{\partial y}) \qquad (1)$$

After the gradient vector field of $f(\vec{r})$ is computed, the isotropic diffusion is performed. The diffusion process is ruled by a partial differential equation set as in [1],

$$\begin{cases} \dfrac{du}{dt} = \mu \nabla^2 u - (u - f_x)(f_x^2 + f_y^2) \\ \dfrac{dv}{dt} = \mu \nabla^2 v - (v - f_y)(f_x^2 + f_y^2) \end{cases} \qquad (2)$$

Here, μ is the regular parameter, u, v are two components of the diffused gradient vector field, f_x and f_y are the two components of $f(\vec{r})$. Initializing u, v with u_0, v_0 in equation (2), the partial differential equation set (2) can be solved iteratively by finite difference technique. We denote by $gvf(\vec{r})$ the diffused gradient vector field obtained by (2) at point $\vec{r}$.

We use isotropic diffusion here because it makes the vectors propagate towards the actual location of the skeleton points. This is very important in order to get the accurate skeleton. Moreover, it is an efficient way of smoothing noise, which makes the extracted skeleton robust under boundary noise.

2.2. Computation of the SSM and its local maxima

To localize the skeleton points from the diffused gradient vector field, we compute a skeleton strength map (SSM) from it. In SSM the value at each point indicates the probability of being a skeleton point. The higher the value at a point, the more probable this point is a skeleton point. It is known that the skeleton points are located where two or more vectors confront. Based on this principle, the skeleton strength map is computed by adopting the formula from [2].

$$SSM(\vec{r}) = \max(0, \sum_{r \in N(\vec{r})} \frac{gvf(\vec{r}) \bullet (\vec{r} - \vec{r}^{\,'})}{\|\vec{r} - \vec{r}^{\,'}\|}), \qquad (3)$$

where $N(\vec{r})$ denotes the eight-neighbors of $\vec{r}$. Each of $\vec{r}$'s eight-neighbors projects its vector to the unit vector pointing from $\vec{r}$ to $\vec{r}^{\,'}$. The intensity of the SSM at $\vec{r}$ is then assigned the value of the sum of projections if the sum is positive. The intuition is that if all $\vec{r}$'s neighbors have gradient vector pointing to it, the intensity of SSM at $\vec{r}$ is high and it is likely to be a skeleton point.

Definition 1: A **local maximum** of *SSM* is a point $\vec{r}$ whose distance transform $SSM(\vec{r})$ satisfies the condition

$$\cdot SSM(\vec{r}) \geq \max_{\vec{r}^{\,'} \in N(\vec{r})} \{SSM(\vec{r}^{\,'})\} \qquad (4)$$

Notice that from the definition, if the equality is achieved, some local maxima may be connected to form a connected region, usually a line, others may be isolated. In order to compute the geodesic curves that define the final skeleton, we select some isolated points from connected local maxima regions to represent them. Those isolated local maxima are defined as critical points in the next subsection.

2.3. Critical point selection and connection

2.3.1. Critical point selection
Definition 2: For a given connected component of local maxima, we select a point with the lowest value of the gradient magnitude $\|\nabla G_\delta(\vec{r}) * dt(\vec{r})\|$. We call it a **critical point**. We also call the endpoints of the connected component **critical points**.

Our definition ensures that critical points correspond to significant visual parts of the object. Therefore, the obtained skeleton contains branches representing all significant visual parts. Notice that in the definition of the critical point, we also include the ends of the connected local maxima regions, because those points usually do not have minimum gradient magnitude. If they are not selected, the skeleton branches may be shortened.

2.3.2. Critical points connection
To connect the critical point set, a distance measure is defined on the surface of function *f*.
Definition 3: Given an 8-connected path $R = \{\vec{r}_1, \vec{r}_2, ... \vec{r}_n\}$, its **gradient length** is defined as $|R|_G = \sum_{i=1}^{n} |f(\vec{r}_i)| \cdot$

The **gradient distance** between two points $\vec{r}$ and $\vec{r}^{\,'}$ is defined as minimum over the gradient lengths of all 8-paths joining them. The 8-path with the smallest gradient distance is called a **gradient path**.

The gradient path corresponds to a geodesic path on the

surface defined by the original distance transform. It is computed with Dijkstra's shortest path algorithm.

We obtain the **skeleton** by connecting the critical points with gradient paths. To begin, we choose the point having the maximum distance transform as the center of the skeleton and connect iteratively all the other critical points to it until all the critical points are connected.

3. RESULTS AND DISCUSSION

In this section, we show several example images and their skeletons extracted by the proposed approach, and compare them with the results based on distance transform only.

Fig. 2 demonstrates the superiority of the propose approach in comparison to computing the skeleton directly on the distance transform map. The result of the proposed method is shown in the first row. The second row demonstrates the computation result based on the distance transform directly. Observe that the lower-left branch of the hand skeleton is missing in Fig. 2(h). As can be seen in (g) no critical points for this region are selected. This is due to the fact that the distance transform value in this region is always increasing, which is quite common for sub-arc like parts due to the nature of the distance transform. Hence true skeleton points find their distance transform always less than some of their 8 neighbors and are not selected as local maxima.

After isotropic diffusion and computation of the SSM, this problem does not occur, because the SSM value depends not on the distance transform but the diffused gradient vector field. As shown in Fig. 2(b), in the lower-left part of the hand, there are some peaks, and therefore, critical points can be selected there as shown in Fig. 2(c). In addition, SSM values tend faster to zero when the distance form the skeleton increases. The final skeleton computed by our method is shown in Fig. 2(d).

A similar result is also shown for the skeleton of the camel in Fig. 3. Again the proposed method is able to compute skeleton branches in all significant visual parts (b), while this is not the case if the computation is based on the distance transform only (c).

From Fig. 4, we can see that this approach yields comparable results as the method describe in Torsello and Hancock [9].

We tested our approach some other images in order to demonstrate its stability, completeness and connectedness. Fig.5 shows skeletons of four different bats. Although the shape variation is great, and the obtained skeletons have similar structure and are positioned accurately.

Fig. 6 shows the skeletons of four rats whose shapes differ in some small boundary deformation. We can see that, this approach yields stable skeletons in this case as well. In all the examples, we choose δ =0.5 and μ=0.07.

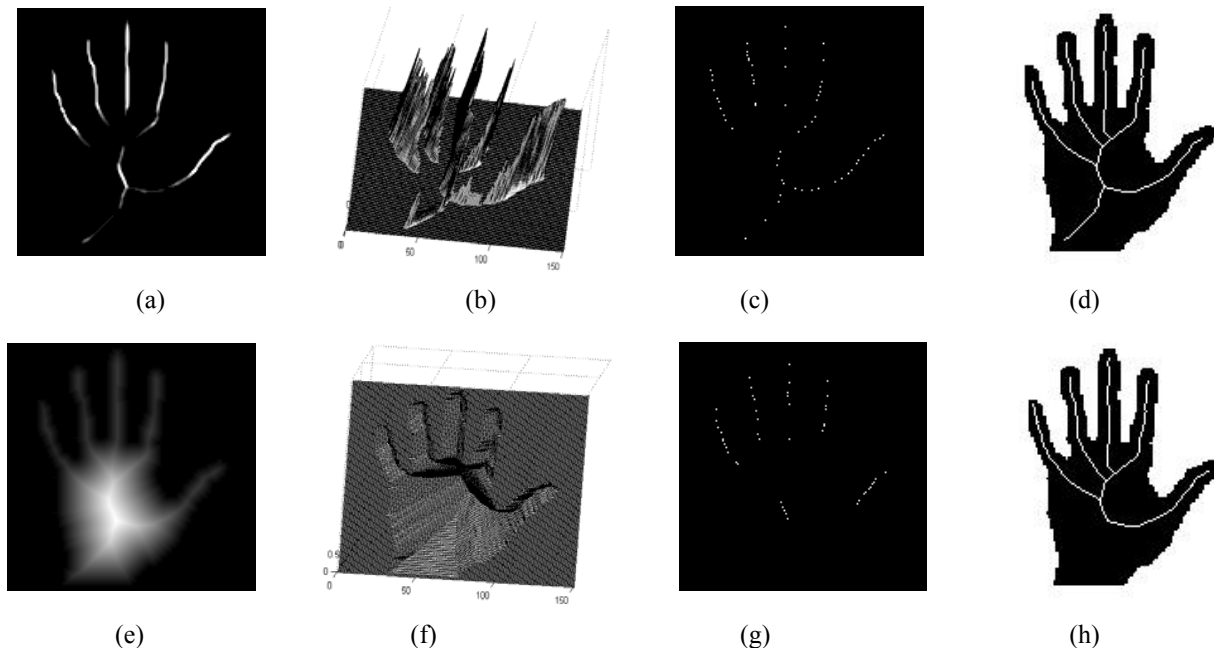| (a) | (b) | (c) | (d) |

| (e) | (f) | (g) | (h) |

Fig. 2 Comparison of results of this approach and the method based on distance transform only. (a) SSM of the hand shown in (d), (b) the SSM surface, (c) is the critical point set selected from the SSM. (d) the final skeleton computed by our method, (e) the distance transform of the hand, (f) the distance transform surface, (f) the critical point set selected from the distance transform, (h) the skeleton computed based on the critical points in (g).
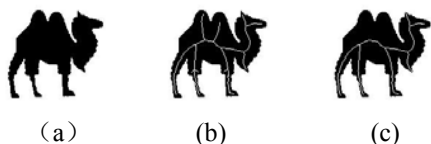
(a)   (b)   (c)

Fig.3 Comparison of results of this approach and the method based on distance transform only. (a) The original figure. (b) The skeleton obtained by this approach (c) The skeleton computed using the distance transform only.
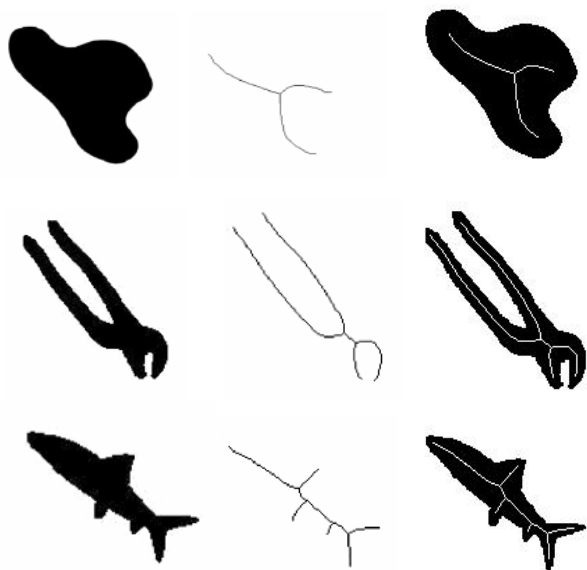

Fig. 4 Left column shows the original images, in middle are the skeletons computed by the method in [9], and the right column shows skeletons obtained by our approach.

Fig. 5 Skeletons of four different bats of very different shape

4. CONCLUSIONS AND FUTURE WORK

We propose a new approach of skeletonization based on isotropic diffusion and computing the SSM of the distance transform. Because of the process of isotropic diffusion and computation of the SSM, this approach overcomes intrinsic drawbacks of methods based on the distance transform related to skeleton connectedness and completeness. Our further work will focus on extending this approach to 3D.
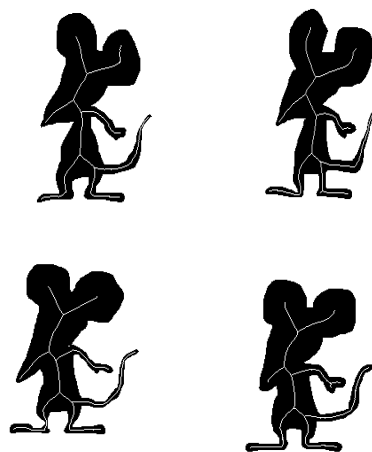

Fig.6 Skeletons of four different rats of similar shape.

5. REFERENCES

[1] C. Xu and J. L. Prince, Snakes, Shapes, and Gradient Vector Flow, *IEEE Trans. Image Processing*, 7(3), pp. 359-369, 1998.

[2] Y. Zeyun and B. Chandrajit, A segmentation-free approach for skeletonization of grayscale images via anisotropic vector diffusion, *Proc. CVPR*, pp. 63-69, 2004.

[3] H. Blum, *A Transformation for Extracting New Descriptors of Shape, Models for the Perception of Speech and Visual Form*, MIT Press, pp. 363-380, 1967.

[4] H. Blum, Biological Shape and Visual Science: Part I. *J. Theoretical Biology*, 38, pp.205-287, 1973.

[5] W.-P. Choi, K.-M. Lam, W.-C. Siu, Extraction of the Euclidean skeleton based on a connectivity criterion, *Pattern Recognition*, 36, pp. 721 - 729, 2003.

[6] F. Leymarie and M. Levine, Simulating the grassfire transaction form using an active Contour model, *IEEE Trans. PAMI,* 14(1), pp. 56 - 75, 1992.

[7] Y. Ge and J. M. Fitzpatrick, On the Generation of Skeletons from Discrete Euclidean Distance Maps, *IEEE Trans. PAMI*, 18(11), pp. 1055-1066, 1996.

[8] K. Siddiqi, S. Bouix, A. Tannenbaum, and S. W. Zucker, The Hamilton–Jacobi skeleton, *Proc. ICCV*, pp. 828–864, Sep.1999.

[9] A. Torsello, and E. R. Hancock, Correcting Curvature-Density Effectsin the Hamilton–Jacobi Skeleton, *IEEE Trans. Image Processing*, 15(4), Apr. 2006

[10] C. Aslan, and S. Tari. An Axis Based Representation for Recognition. *Proc. ICCV*, 2005.

[11] X. Bai, L. J. Latecki, and W. Y. Liu, Skeleton Pruning by Contour Partitioning with Discrete Curve Evolution, *IEEE Trans. PAMI,* 29(3), pp.449-462, 2007.

[12] N. Cornea, D. Silver, X. Yuan, and R. Balasubramanian, Computing Hierarchical Curve-Skeletons of 3D Objects, *The Visual Computer*, October 2005.